Desalination and Water Treatment
www.deswater.com

doi: 10.1080/19443994.2015.1086892

57 (2016) 17454–17462
August

Taylor & Francis
Taylor & Francis Group

Magnetic iron oxide nanoparticles modified by methyl trioctyl ammonium chloride as an adsorbent for the removal of erythrosine from aqueous solutions

N. Pourreza*, H. Parham, M.A. Pourbati

Department of Chemistry, College of Science, Shahid Chamran University, Ahvaz, Iran, Tel. +98 6133331042; Fax: +98 6133337009; emails: npourreza@scu.ac.ir (N. Pourreza), hoparham@yahoo.com (H. Parham), ma.pourbati@yahoo.com (M.A. Pourbati)

Received 18 August 2014; Accepted 13 August 2015

ABSTRACT

In this research work, the removal of erythrosine by magnetic iron oxide nanoparticles modified by methyl trioctyl ammonium chloride (Aliquat 336) was investigated. Fourier transform infrared and transmission electron microscopy were applied for surface characterization of modified iron oxide nanoparticles. In order to obtain the maximum removal efficiency, effects of pH, amount of adsorbent, electrolyte, stirring time, temperature, and interfering ions were investigated. It was found that the adsorption equilibrium was attained after 2 min of stirring time. Langmuir, Freundlich, Temkin, and Dubinin–Radushkevich isotherm models were applied to fit adsorption equilibrium data. The best-fitted data was obtained with the Langmuir model and the adsorbent capacity was 149.2 mg g^{-1}. Kinetic studies indicated that the adsorption process was described better by pseudo-second-order model. This method was successfully applied for the removal of erythrosine from water samples.

Keywords: Erythrosine; Magnetic iron oxide nanoparticles; Aliquat 336; Removal

1. Introduction

The extensive use of dyes often brings pollution problems in the form of colored wastewater [1]. Synthetic dyes are a large group of organic chemical compounds that are discarded by various industries such as textile, food, leather, plastic, pulp, and paper to their effluents. The discharge of colored wastes into streams not only affects their esthetic nature but also interferes with the transmission of sunlight into streams and therefore reduces photosynthetic action [2]. Large amounts of dyes are continuously entering the water systems from industries due to improper processing and dyeing methods [3]. Some of these dyes are a potential risk to human health in excess amount and may present an ecotoxic hazard [4–6]. Hence, the removal of dyestuff from waste effluents becomes environmentally important.

Considerable research has been done on color removal from wastewater. Among different techniques, adsorption is a more attractive method for the removal of dyes due to its merits of simplicity, high efficiency, and low cost. The adsorption process provides an attractive treatment, especially if the adsorbent is inexpensive and readily available. In this regard, some work has been performed to remove erythrosine dye from water by various adsorbent including activated carbon [7], biosorbents [8–11] and

*Corresponding author.

nanoadsorbent [12]. Nanotechnology, as the other method, is quickly developing and has found application in water treatment. At the same time, magnetic nanoparticles have attracted considerable interest as the new adsorbents due to their large specific surface area, small diffusion route, high separation efficiency, easy in synthesis, and low cost [13]. Recently, magnetic iron oxide nanoparticles (MIONPs) have shown extensive applications as solid-phase adsorbent for the removal of different types of pollutants such as dyes and heavy metals [14–21]. Nanosized magnetic iron oxide particles have found a wide range of applications in ferrofluids, high-density information storage, magnetic resonance imaging, biological cell labeling, separation of biochemicals, targeting, and drug delivery. For many of these applications, surface modification of nanosized magnetic particles is a key of challenge. In general, surface modification can be accomplished by physical or chemical adsorption of the desired molecules to coat the surface, depending on the specific applications [22,23]. Several reports have been published on using magnetic nanoparticles for removal, separation, and determination of metals ions [24], organic compounds [25], and dyes [26].

Erythrosine (Fig. 1) is a xanthene class, water-soluble cherry-pink red synthetic coal dye, which is used for dyeing a variety of materials, such as wool, silk, and nylon. Erythrosine is one of the widely used colorant in drugs and cosmetics and is also used to color a large variety of food stuffs such as biscuits, chocolates, sweets, tinned cherries, fruits, luncheon meat, salmon spread, stuffed olives, chewing gums, jellies, and ice creams. Erythrosine is highly toxic to mankind and can lead to many diseases including carcinogenicity. Erythrosine is a water-soluble dye with high solubility, so it is difficult to remove it by common chemical treatments. Therefore, monitoring and eliminating erythrosine from wastewater is an important subject due to its potential toxicity and pathogenicity for the human health and animals [7–9,11].

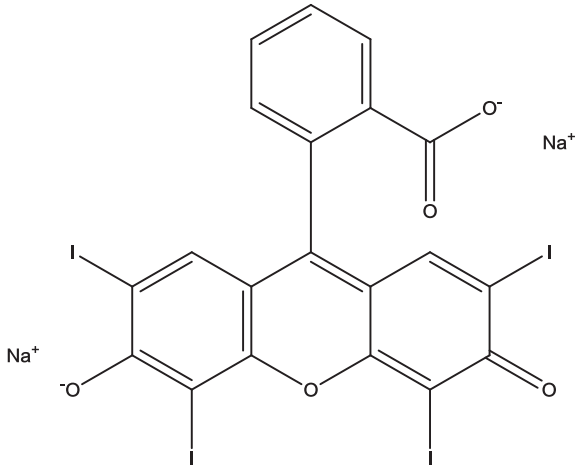

Fig. 1. The chemical structure of erythrosine.

In this paper, MIONPs were modified by methyl trioctyl ammonium chloride (Aliquat 336) (MIONPs–Aliquat) and used as a new solid-phase adsorbent for the removal of erythrosine. The dependence of removal procedure on the concentration of dye, pH, contact time, and adsorbent dose was investigated and optimal conditions for the adsorption were established. At these conditions, the results were fitted to Langmuir, Freundlich, Temkin, and Dubinin–Radushkevich. MIONPs–Aliquat adsorbent was employed for the removal of erythrosine from water samples.

2. Experimental

2.1. Apparatus

A GBC Model Cintra 101 UV–visible spectrophotometer (Sidney, Australia) was used for recording the absorption spectra and absorbance measurements were carried out with a JASCO model 7850 UV–visible spectrophotometer (Tokyo, Japan) using 1-cm glass cells. Transmission electron microscopy (TEM) images were recorded on TEM micrographs (906E, LEO, Germany). Infrared spectra were obtained using a Bomem FT-IR spectrometer (Canada) to identify the functional groups and chemical bonding of the coated materials. A Metrohm digital pH meter Model 632 (Herisau, Switzerland) with a combined glass electrode was used to measure the pH values. A magnet (1.2 T, $10 \times 5 \times 2$ cm) was used for settlement of magnetic nanoparticles.

2.2. Materials and solutions

All chemicals and reagents were of analytical grade purity. Erythrosine, ethanol (96% v/v), ammonia solution (25% w/w), hydrochloric acid ($d = 1.18$, 37% w/w), $FeCl_3$, and $FeCl_2$ $4H_2O$ were purchased from Merck (Darmstadt, Germany) and were used without further purification processes. Methyl trioctyl ammonium chloride (Aliquat 336) was obtained from Sigma (St. Loius, MO, USA). 100 mg L^{-1} stock solution of erythrosine was prepared by dissolving 0.1 of the powder in water and diluting to 1,000 mL in a volumetric flask. Phosphate buffer solution (pH 7) was prepared by adding appropriate amounts of sodium hydroxide (Merck) to 0.1 M phosphoric acid (Merck) solution and adjusting the pH to 7 by a pH meter.

2.3. Synthesis of modified iron oxide magnetic nanoparticles

The synthesis and modification of MIONPs by Aliquat 336 were carried out simultaneously. Fe_3O_4 nanoparticles were prepared by the co-precipitation of Fe^{2+} and Fe^{3+} ions and slight modification of the previous method [25]. For this purpose, 3.2 g of $FeCl_2{\cdot}4H_2O$ and 5.2 g of $FeCl_3$ were weighed and transferred to a 500-mL beaker. Then 320 mL of water was added and stirred on a heater stirrer at 80˚C for 1 h. Afterward, 0.25 g of Aliquat 336 was dissolved in 40 mL of acetone and added to this solution and stirred on a heater stirrer at 80˚C for another hour. After this period, 40 mL of ammonia solution was added dropwise and stirred on a heater stirrer at 80˚C for another hour. The solution was placed on a magnet and the supernatant solution was discarded. The modified nanoparticles were washed with water five times to remove excess ammonia and stored for further use. Fig. 2 shows the scheme for the synthesis of MIONPs–Aliquat and removal procedure of erythrosine.

2.4. Removal and separation procedure

Adsorption experiments of erythrosine by adsorbent were conducted using the batch method. 0.2 g of wet MIONPs–Aliquat (equivalent to 0.020 g of dried particles) was added to 50 mL solution of erythrosine (30 μg mL^{-1}) containing 2 mL of phosphate buffer (pH 7). The solution was stirred vigorously for 2 min by a glass rod, and then the solid phase was separated from solution using a magnet. The erythrosine concentration in the supernatant was determined spectrohotometrically by measuring the absorbance of the sample solution at 530 nm. The percent removal of erythrosine by the adsorbent was calculated according to the Eq. (1):

$$R(\%) = \frac{(C_0 - C_t)}{C_0} \times 100 \quad (1)$$

where R is the removal efficiency of the erythrosine, C_0 and C_t represent the initial and final (after adsorption) dye concentrations in μg mL^{-1}, respectively.

3. Results and discussion

The preliminary experiments showed that the anionic dye erythrosine is not adsorbed by bare MIONPs particles very well (only 6%). Therefore, it was decided to modify its surface by Aliquat 336 which is a quaternary ammonium salt for better adsorption. The methyl trioctyl ammonium ion (cation of Aliquat 336) could form an ion pair with anionic dye erythrosine and remove it from aqueous solution.

The UV–vis absorption spectrum of erythrosine was recorded (Fig. 3) and showed that the maximum absorption occurs at 530 nm. Thus, all the absorbance measurements were carried out at this wavelength.

3.1. Characteristics of modified iron oxide nanoparticles

The morphology of MIONPs and MIONPs–Aliquat was observed by TEM images as shown in Fig. 4(A) and (B). It is observed in Fig. 4 that the modified MIONPs (B) are more dispersed with well-shaped particles (approximate size of 20–80 nm) due to more

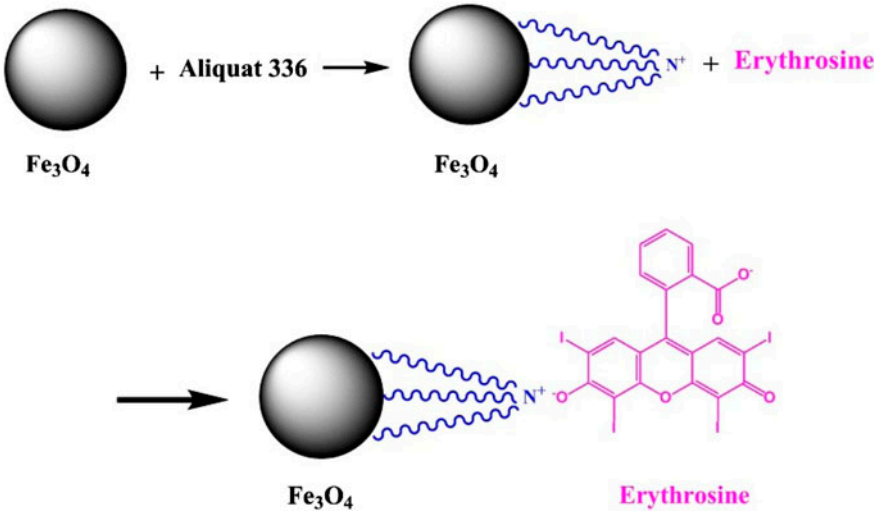

Fig. 2. Synthesis of MIONPs–Aliquat and removal procedure.

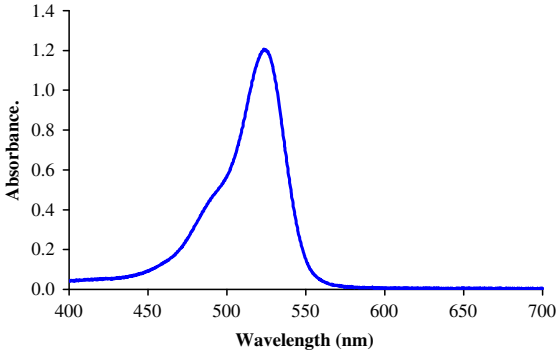

Fig. 3. The UV–vis absorption spectrum of erythrosine.

positive surface occupied by the large quaternary ammonium ion than unmodified MIONPs particles (A) which are more aggregated.

The Fourier transform infrared (FTIR) spectra of pure MIONPs (A) and MIONPs–Aliquat (B) are presented in Fig. 5. The major peaks in Fig. 5 can be assigned as follows: the adsorption band around ~557 cm^{-1}, revealing the stretching vibration of Fe–O band in both spectra, and the peak at ~1,635 cm^{-1} is attributed to C–N bending vibrations, the peak at 1,397 cm^{-1} are attributed to CH_3 bending vibrations and the peak at ~1,120 cm^{-1} are attributed to C–N stretching vibrations of Aliquat 336. By overlaying these FTIR spectra, the spectral similarities are observed and indicate that MIONPs surface was well modified by Aliquat 336.

3.2. Effect of pH on the adsorption

The pH value plays an important role in the adsorption process of the dye molecules and particularly on the adsorption capacity. In order to evaluate the influence of this parameter on the adsorption of the erythrosine dye, the experiments were carried out in the pH range of 3–9. The pH of the solutions was adjusted by NaOH and HCl using a pH meter. The obtained results are shown in Fig. 6. The study of the effect of pH on the adsorption of erythrosine by 0.2 g of damp MIONPs–Aliquat at 25°C showed that the percent removal of erythrosine remains constant in the pH range of 6–9. Acid conditions are not favorable because iron oxide nanoparticles are dissolved. Thus, the pH value of 7 was used as optimum pH for further works. Phosphate buffer pH 7 was found to be suitable for adjusting pH and 2 mL of this buffer was added to 50 mL solutions containing 30 μg mL^{-1} of erythrosine for maintaining the pH at this value.

3.3. Effect of the Aliquat 336 amount

The influence of Aliquat amount (in the range of 0.10–0.30 g) in the modification of iron oxide nanoparticles for the removal of the dye was studied. The results revealed that by increasing the amount of Aliquat 336 up to 0.20 g, the removal efficiency was increased and remained nearly constant above that. Therefore, 0.25 g was chosen as optimum amount for further experiments.

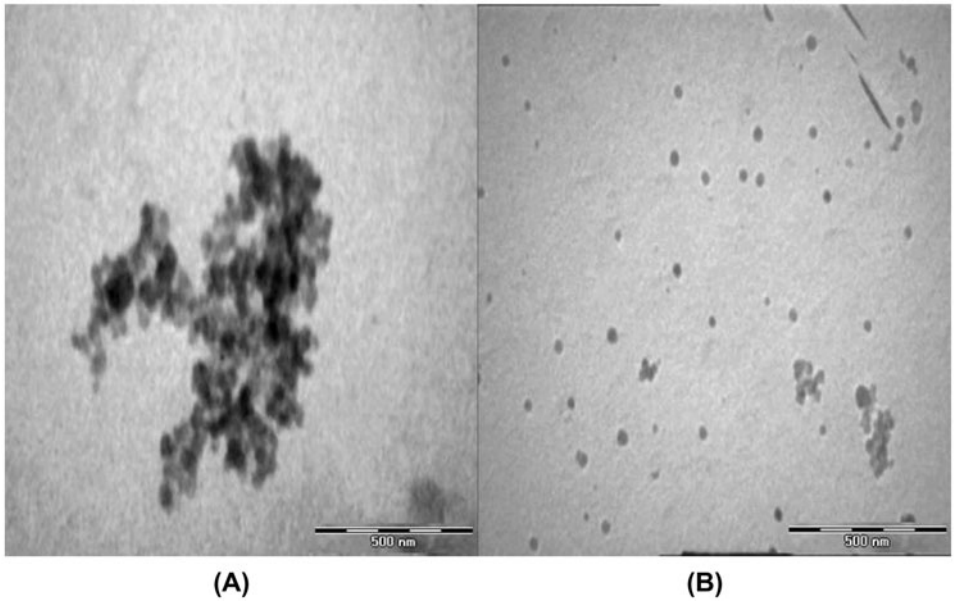

Fig. 4. TEM image of (A) MIONPs and (B) MIONPs–Aliquat.

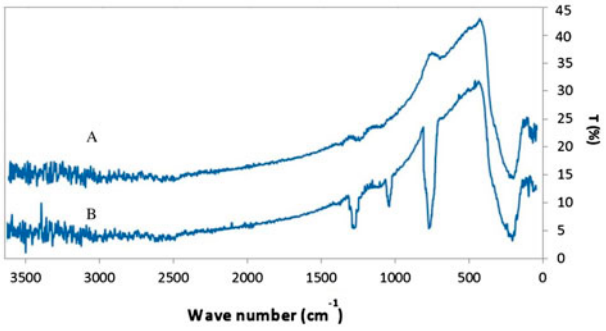

Fig. 5. FT-IR spectra of (A) MIONPs and (B) MIONPs–Aliquat adsorbent.

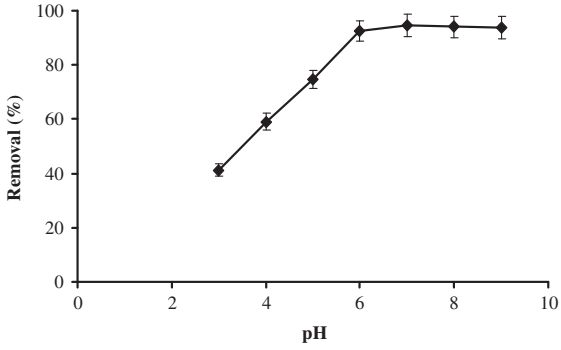

Fig. 6. Effect of pH on the removal of 30 mg L^{-1} of erythrosine by 0.2 g of MIONPs–Aliquat adsorbent at pH 7.

3.4. Effect of amount of adsorbent

The effect of various amounts of MIONPs–Aliquat adsorbent for the quantitative removal of erythrosine from 50 mL solution (30 μg mL^{-1}) at pH 7 was investigated. The results shown in Fig. 7 indicate that an increase in the amount of the IONPs leads to an increase in the removal efficiencies. However, above 0.15 g of MIONPs–Aliquat, the adsorption of the dye and its removal was almost constant. Thus, 0.2 g of the adsorbent was selected as optimum value.

3.5. Effect of salt concentration

Ionic strength (salt concentration) influences both electrostatic and non-electrostatic interactions between the adsorbate and the adsorbent surface. Since NaCl is usually used as a stimulator in dyeing processes and ionic strength affects the activity coefficients for OH^-, H_3O^+, and specifically absorbable ions [6], hence the influence of NaCl on the removal of erythrosine was examined in the concentration range of 0.06–0.18 mol L^{-1}. The obtained results revealed that the

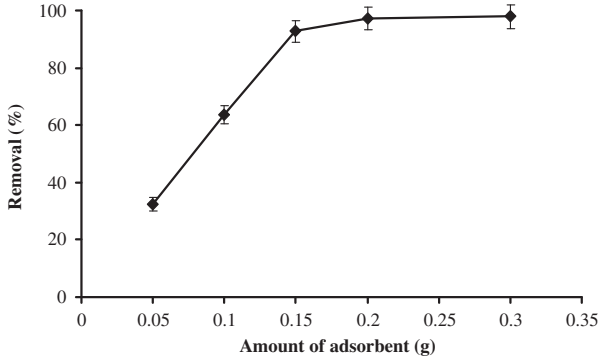

Fig. 7. Effect of adsorbent dose on the removal of 30 mg L^{-1} of erythrosine by MIONPs–Aliquat adsorbent at pH 7.

removal efficiency was nearly constant by increasing the salt concentration, indicating that the presence of an electrolyte does not have a significant effect on the removal process.

3.6. Effect of equilibration temperature

The temperature dependence of erythrosine adsorption onto MIONPs–Aliquat adsorbent was studied at a constant initial concentration of 30 μg mL^{-1} and pH 7. This study showed that temperature above 20°C had no significant effect on the adsorption of erythrosine and below that there was a small change in the removal of erythrosine by MIONPs–Aliquat. Therefore, the experiments were easily conducted at room temperature (25 ± 1°C).

3.7. Effect of contact time

The effect of contact time on the adsorption of erythrosine was investigated to determine the optimum time. Fig. 8 shows the adsorption of erythrosine as a function of contact time for different dye concentrations. Rapid adsorption kinetics can be obviously seen within the first 60 s and the adsorption of erythrosine increased by contact time up to 90 s and remained contact after this time. Hence, 120 s (2 min) was selected as optimum contact time. This rapid adsorption process could be due to the availability of the active surface of the adsorbent.

3.8. Adsorption isotherm

The equilibrium isotherms using Langmuir, Freundlich, Temkin, and Dubinin–Radushkevich isotherm models for erythrosine adsorption by

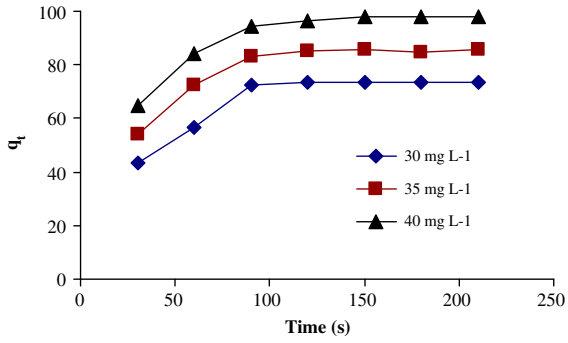

Fig. 8. The effect of time on the removal of erythrosine by 0.2 g of MIONPs–Aliquat adsorbent at pH 7.

MIONPs–Aliquat in phosphate buffer solution (pH 7) at 25℃ were prepared [27,28].

The linear form of the Langmuir model is written as Eq. (2):

$$\frac{C_e}{q_e} = \frac{1}{K_L q_m} + \frac{C_e}{q_m} \tag{2}$$

where q_e is the equilibrium adsorption amount of erythrosine (mg g^{-1}), C_e is the equilibrium erythrosine concentration in the solution (μg mL^{-1}), q_m is the maximum adsorption amount of erythrosine per gram of adsorbent (mg g^{-1}), and K_L is the Langmuir adsorption equilibrium constant (L mg^{-1}).

A plot of C_e/q_e against C_e yielded a straight line with the following Eq. (3):

$$C_e/q_e = 0.0066\, C_e + 0.0075 \quad (r = 0.9987) \tag{3}$$

The features of Langmuir isotherm can also be expressed in terms of a dimensionless factor called equilibrium parameter, R_L which is defined as Eq. (4):

$$R_L = \frac{1}{1 + K_L C_0} \tag{4}$$

where C_0 is the initial metal concentration (mg L^{-1}). The R_L values may be used to predict if an adsorption system is favorable or unfavorable. The value of R_L indicates the type of isotherm to be favorable if $0 < R_L < 1$, unfavorable if $R_L > 1$, linear if $R_L = 1$, or irreversible ($R_L = 0$). Since the R_L values calculated from the obtained results are between 0 and 1 (0.013–0.097) for the adsorption of erythrosine onto MIONPs–Aliquat, the adsorption process is considered favorable.

The Freundlich isotherm expresses adsorption at multilayer and on energetically heterogeneous surfaces. It is an empirical equation suitable for high and middle range of solute concentration but not for low concentrations. Freundlich model in linear form is given as Eq. (5) [27]:

$$\log q_e = \log K_F + \frac{1}{n} \log C_e \tag{5}$$

where q_e designates the amount of erythrosine adsorbed at equilibrium in mg g^{-1}, C_e is the solute equilibrium concentration in mg L^{-1}, K_F is a constant related to the adsorption capacity, and $1/n$ is an empirical parameter related to the adsorption intensity, which varies with the heterogeneity of material.

Adsorption data were also correlated with Freundlich model and a curve of log q_e vs. log C_e was constructed. The correlation coefficient was found to be 0.9734.

The Temkin isotherm describes the adsorption behavior on heterogeneous surfaces and is expressed by a linear Eq. (6):

$$q_e = B_T \ln K_T + B_T \ln C_e \tag{6}$$

where $B_T = RT/b_T$, T is the absolute temperature in K and R is the gas constant (8.314 J mol^{-1} K^{-1}, K_T is the equilibrium binding constant (L mg^{-1}) and B_T is related to the heat of adsorption.

The Dubinin–Radushkevich (D–R) model does not assume a homogeneous surface and it is used to distinguish between the physical and chemical adsorptions [28]. The Dubinin–Radushkevich equation is given by Eq. (7):

$$\ln q_e = \ln q_m - k\, \varepsilon^2 \tag{7}$$

where q_e and q_m have the same meaning as before, k (-mol^2 J^{-2}) is a constant related to the adsorption energy, and ε is given by Eq. (8):

$$\varepsilon = RT \ln\left(1 + \frac{1}{C_e}\right) \tag{8}$$

where R is the gas constant (J mol^{-1} K^{-1}) and T is the absolute temperature in K. The constant k gives the mean free energy E (kJ mol^{-1}) of sorption per molecule of the sorbate given as the Eq. (9):

Table 1
Comparison of the Langmuir, Freundlich, Temkin, and Dubinin–Radushkevich isotherm models for the adsorption of erythrosine on MIONPs–Aliquat

Isotherm model	Parameter	Value
Langmuir isotherm	q_m (mg g^{-1})	149.2
	K_L (L mg^{-1})	0.93
	r	0.9982
Freundlich isotherm	K_F (mg g^{-1})	86.19
	n	5.58
	r	0.9734
Temkin isotherm	B_T (J mol^{-1})	19.44
	K_T (L g^{-1})	84.80
	r	0.9855
Dubinin–Radushkevich	q_m (mg g^{-1})	131.76
	K (mol^2 kJ^{-2})	0.141
	r	0.9514
	E (kJ mol^{-1})	1.8831

$$E = 1/\sqrt{2k} \tag{9}$$

where E is used to estimate the type of adsorption process. If $E < 8$ kJ mol^{-1}, adsorption process is of a physical nature, whereas if value $8 < E < 16$ kJ mol^{-1}, the adsorption process can be explained by ion exchange mechanism.

The slope of the plot of ln q_e vs. ε^2 gives k and the intercept yields the adsorption capacity, q_m (mg g^{-1}).

The calculated constant values of the Langmuir, Freundlich, Temkin, and Dubinin–Radushkevich isotherms along with their correlation coefficients are given in Table 1.

It was observed that the experimental data are better fitted with the Langmuir isotherm ($r = 0.9982$) for the adsorption of erythrosine on the MIONPs–Aliquat. The maximum monolayer adsorption capacity, q_m, obtained from Langmuir model is 149.2 mg g^{-1} for erythrosine. The calculated value of D–R model constant shows that the value of E was 1.8831 kJ mol^{-1} which is <8 kJ mol^{-1} indicating that the adsorption process has a physical nature.

3.9. Adsorption kinetics

The kinetic models were used to predict the variation of adsorbed erythrosine with time using MIONPs–Aliquat. The rate constants of chemical adsorption were determined using the equations of the pseudo-first-order and pseudo-second-order models. Pseudo-first-order model is one of the most widely used procedures for the adsorption of a solute from aqueous solution [27]. The pseudo-first-order kinetic model of Lagergren is given as follows:

$$\log(q_e - q_t) = \log q_e - \frac{K_1 t}{2.303} \tag{10}$$

where q_e and q_t are the amounts of erythrosine adsorbed onto MIONPs–Aliquat (mg g^{-1}) at equilibrium and at time t, respectively, and K_1 (1/min) is first-order rate constant for adsorption. The rate constant, k_1, can be calculated from the plots of log ($q_e - q_t$) vs. t. Pseudo-second-order kinetics may be expressed as the following equation:

$$\frac{t}{q_t} = \frac{1}{k_2 q_e^2} + \frac{t}{q_e} \tag{11}$$

where k_2 is the rate constant of the second-order adsorption (g mg^{-1} min). The straight-line plots of t/q_t against t have been tested to obtain rate parameters.

The pseudo-first-order and pseudo-second-order kinetic models for erythrosine removal by MIONPs–Aliquat were investigated using the above equations. The results indicate that the adsorption of erythrosine on MIONPs–Aliquat is not fitted to a first-order model and correlation coefficients of about 0.1 were obtained. However, the correlation coefficients for the second-order kinetic model were higher than 0.999 indicating the applicability of this kinetic model of the adsorption process of erythrosine on MIONPs–Aliquat adsorbent.

3.10. Effect of different ions

The optimum experimental conditions which have been described were used to study the effect of some ions and two dyes (congo red and malachite green) on the adsorption process. The maximum acceptable error was ±5%. The obtained results shown in Table 2 indicate that most ions are tolerable at high concentrations.

3.11. Removal of erythrosine from aqueous solutions

The removal procedure was successfully applied to remove erythrosine from spiked aqueous solutions.

Table 2
Effect of interfering ions and dyes on the removal of 30 μg mL^{-1} of erythrosine

Interfering ion	Tolerance limit (μg mL^{-1})
Na^+, K^+, Ag^+, Cu^{2+}, Ca^{2+}, Mg^{2+}, NH_4^+, F^-, Cl^-, I^-, NO_3^-, SO_4^{2-}, CO_3^{2-}, $C_2O_4^{2-}$, Br^-	500
Mn^{2+}, Fe^{3+}, Al^{3+}, Ni^{2+}, Pb^{2+}	20
Congo red	25
Malachite green	3

Table 3
Removal of erythrosine from spiked aqueous solutions

Sample	Present concentration (mg L^{-1})	Removal (%)
Tap water	30	97.4
Karoon river	30	97.1
Maroon river	30	96.6

The results of this investigation are shown in Table 3. As it is observed, quantitative recoveries (>95%) are obtained for all the samples.

4. Conclusion

The work presented in this manuscript describes a new adsorbent for the removal of erythrosine from aqueous solutions. The present investigation shows that MIONPs–Aliquat is a capable low-cost adsorbent for the removal of erythrosine from aqueous solutions. MIONPs–Aliquat adsorbent was easily prepared by a chemical co-precipitation method and exhibited high adsorption capacity and fast adsorption rates for the removal of erythrosine. The nanoparticles of adsorbent were characterized using TEM and FTIR, also the adsorption behavior was described by Langmuir isotherm. A comparison between the proposed adsorbent with some of the previously reported adsorbents for the removal of erythrosine indicate that the removal performance of the proposed method for erythrosine is more satisfactory [7–9,12]. Finally, the iron oxide nanoparticles modified by Aliquat could be a promising candidate of high efficiency, low cost, and facile separation under magnetic separation field.

Acknowledgment

The authors gratefully acknowledge Shahid Chamran University Research Council for financial support of this work (Grant 1394). The financial support of the Iranian Nanotechnology Initiative Council is also appreciated.

References

[1] A. Ergene, K. Ada, S. Tan, H. Katırcıoğlu, Removal of Remazol Brilliant Blue R dye from aqueous solutions by adsorption onto immobilized Scenedesmus quadricauda: Equilibrium and kinetic modeling studies, Desalination 249 (2009) 1308–1314.
[2] C. Namasivayam, D. Prabha, M. Kumutha, Removal of direct red and acid brilliant blue by adsorption on to banana pith, Bioresour. Technol. 64 (1998) 77–79.
[3] A. Mittal, J. Mittal, A. Malviya, D. Kaur, V.K. Gupta, Adsorption of hazardous dye crystal violet from wastewater by waste materials, J. Colloid Interface Sci. 343 (2010) 463–473.
[4] M. Iram, C. Guo, Y. Guan, A. Ishfaq, H. Liu, Adsorption and magnetic removal of neutral red dye from aqueous solution using Fe_3O_4 hollow nanospheres, J. Hazard. Mater. 181 (2010) 1039–1050.
[5] L. Fan, Y. Zhang, C. Luo, F. Lu, H. Qiu, M. Sun, Synthesis and characterization of magnetic β-cyclodextrin–chitosan nanoparticles as nano-adsorbents for removal of methyl blue, Int. J. Biol. Macromol. 50 (2012) 444–450.
[6] M. Ghaedi, H. Hossainian, M. Montazerozohori, A. Shokrollahi, F. Shojaipour, M. Soylak, M.K. Purkait, A novel acorn based adsorbent for the removal of brilliant green, Desalination 281 (2011) 226–233.
[7] Y.S. Al-Degs, R. Abu-El-Halawa, S.S. Abu-Alrub, Analyzing adsorption data of erythrosine dye using principal component analysis, Chem. Eng. J. 191 (2012) 185–194.
[8] V.K. Gupta, A. Mittal, L. Kurup, J. Mittal, Adsorption of a hazardous dye, erythrosine, over hen feathers, J. Colloid Interface Sci. 304 (2006) 52–57.
[9] R. Jain, S. Sikarwar, Adsorptive removal of erythrosine dye onto activated low cost de-oiled mustard, J. Hazard. Mater. 164 (2009) 627–633.
[10] G.J. Copello, A.M. Mebert, M. Raineri, M.P. Pesenti, L.E. Diaz, Removal of dyes from water using chitosan hydrogel/SiO_2 and chitin hydrogel/SiO_2 hybrid materials obtained by the sol–gel method, J. Hazard. Mater. 186 (2011) 932–939.
[11] A. Mittal, J. Mittal, L. Kurup, A.K. Singh, Process development for the removal and recovery of hazardous dye erythrosine from wastewater by waste materials- bottom ash and de-oiled soya as adsorbents, J. Hazard. Mater. 138 (2006) 95–105.
[12] M. Roosta, M. Ghaedi, A. Daneshfar, S. Darafarin, R. Sahraei, M.K. Purkait, Simultaneous ultrasound-assisted removal of sunset yellow and erythrosine by ZnS: Ni nanoparticles loaded on activated carbon: Optimization by central composite design, Ultrason. Sonochem. 21 (2014) 1441–1450.
[13] N. Pourreza, S. Rastegarzadeh, A. Larki, Nano-TiO_2 modified with 2-mercaptobenzimidazole as an efficient adsorbent for removal of Ag(I) from aqueous solutions, J. Ind. Eng. Chem. 20 (2014) 127–132.
[14] R. Rakhshaee, M. Panahandeh, Stabilization of a magnetic nano-adsorbent by extracted pectin to remove methylene blue from aqueous solution: A comparative studying between two kinds of cross-likened pectin, J. Hazard. Mater. 189 (2011) 158–166.
[15] T. Türk, İ. Alp, Arsenic removal from aqueous solutions with Fe-hydrotalcite supported magnetite nanoparticle, J. Ind. Eng. Chem. 20 (2014) 732–738.
[16] Y.J. Tu, C.F. You, C.K. Chang, S.L. Wang, XANES evidence of arsenate removal from water with magnetic ferrite, J. Environ. Manage. 120 (2013) 114–119.
[17] S. Unal Yesiller, A.E. Eroğlu, T. Shahwan, Removal of aqueous rare earth elements (REEs) using nano-iron based materials, J. Ind. Eng. Chem. 19 (2013) 898–907.
[18] K. Song, W. Kim, C.Y. Suh, D. Shin, K.S. Ko, K. Ha, Magnetic iron oxide nanoparticles prepared by electrical wire explosion for arsenic removal, Powder Technol. 246 (2013) 572–574.

[19] J.H. Deng, X.R. Zhang, G.M. Zeng, J.L. Gong, Q.Y. Niu, J. Liang, Simultaneous removal of Cd(II) and ionic dyes from aqueous solution using magnetic graphene oxide nanocomposite as an adsorbent, Chem. Eng. J. 226 (2013) 189–200.
[20] H. Parham, B. Zargar, R. Shiralipour, Fast and efficient removal of mercury from water samples using magnetic iron oxide nanoparticles modified with 2-mercaptobenzothiazole, J. Hazard. Mater. 205–206 (2012) 94–100.
[21] Y.R. Zhang, S.L. Shen, S.Q. Wang, J. Huang, P. Su, Q.R. Wang, B.X. Zhao, A dual function magnetic nanomaterial modified with lysine for removal of organic dyes from water solution, Chem. Eng. J. 239 (2014) 250–256.
[22] M. Takafuji, S. Ide, H. Ihara, Z. Xu, Preparation of poly(1-vinylimidazole)-grafted magnetic nanoparticles and their application for removal of metal ions, Chem. Mater. 16 (2004) 1977–1983.
[23] H. Zhu, M. Zhang, Y. Liu, L. Zhang, R. Han, Study of congo red adsorption onto chitosan coated magnetic iron oxide in batch mode, Desalin. Water Treat. 37 (2012) 46–54.
[24] A. Uheida, M. Iglesias, C. Fontàs, M. Hidalgo, V. Salvadó, Y. Zhang, M. Muhammed, Sorption of palladium(II), rhodium(III), and platinum(IV) on Fe_3O_4 nanoparticles, J. Colloid Interface Sci. 301 (2006) 402–408.
[25] H. Parham, B. Zargar, M. Rezazadeh, Removal, preconcentration and spectrophotometric determination of picric acid in water samples using modified magnetic iron oxide nanoparticles as an efficient adsorbent, Mater. Sci. Eng. 32 (2012) 2109–2114.
[26] V. Rocher, J.M. Siaugue, V. Cabuil, A. Bee, Removal of organic dyes by magnetic alginate beads, Water Res. 42 (2008) 1290–1298.
[27] M. Ghaedi, N. Taghavimoghadam, S. Naderi, R. Sahraei, A. Daneshfar, Comparison of removal of bromothymol blue from aqueous solution by multiwalled carbon nanotube and Zn(OH)2 nanoparticles loaded on activated carbon: A thermodynamic study, J. Ind. Eng. Chem. 19 (2013) 1493–1500.
[28] M. Ravanan, M. Ghaedi, A. Ansari, F. Taghizadeh, D. Elhamifar, Comparison of the efficiency of Cu and silver nanoparticle loaded on supports for the removal of Eosin Y from aqueous solution: Kinetic and isotherm study, Spectrochim. Acta Part A 123 (2014) 467–472.